Sodium under pressure: bcc to fcc structural transition and pressure-volume relation to 100 GPa

M. Hanfland,[1] I. Loa,[2] and K. Syassen[2,*]
[1]*European Synchrotron Radiation Facility, BP 220, F-38043 Grenoble, France*
[2]*Max-Planck-Institut für Festkörperforschung, Heisenbergstrasse 1, D-70569 Stuttgart, Germany*
(Received 27 November 2001; published 13 May 2002)

The pressure-volume relation of sodium is measured up to 100 GPa using high-resolution angle-dispersive synchrotron x-ray diffraction. At a pressure of 65(1) GPa Na is found to undergo a structural phase transition from a body-centered to a face-centered-cubic modification. Total-energy calculations of Na under pressure are performed using the full-potential linearized augmented plane-wave method. The calculated pressure-volume relations and the bcc-fcc transition pressure are compared to the experimental results.

DOI: 10.1103/PhysRevB.65.184109 PACS number(s): 61.50.Ks, 61.66.Bi, 64.70.Kb, 62.50.+p

I. INTRODUCTION

Recently, attention was drawn to the high-pressure behavior of light alkali metals. Neaton and Ashcroft[1] predicted, on the basis of *first-principles* band-structure theory, that dense Li may undergo structural phase transitions to low-symmetry structures with semimetallic or semiconducting properties. These effects are related to a pressure-driven redistribution of *s*- and *p*-orbital characters in the occupied part of the conduction band.[2,3] Siringo *et al.*[4] considered a different scenario, which could lead to an insulating (charge-density wave) ground state in light alkalis at intermediate densities. The calculations for Li by Neaton and Ashcroft stimulated several recent experimental studies of Li under pressure.[5–9] In the case of sodium, the prototype of a nearly free-electron metal, the effect of pressure on the electronic properties was already studied at a very early stage of the quantum theory of solids.[10] Several interesting aspects of compressed sodium were addressed in recent theoretical work,[4,11–13] among them the anomalous pressure dependence of elastic properties and possible structural instabilities of common close-packed structures at pressures above 100 GPa.

On the experimental side, the pressure-temperature phase diagram of Na was explored up to about 50 GPa. Upon cooling at very low pressures (<0.2 GPa) Na undergoes a partial transformation from the bcc structure to a faulted hexagonal structure.[14–21] At room temperature bcc Na was studied by volumetric methods[22–25] and ultrasonic experiments.[26,27] The melting point of Na increases with pressure from 380 K to $\sim$650 K at 12 GPa.[28] Reduced shock data ($T=298$ K) cover pressures up to several tens of gigapascal;[29] these are mostly derived from liquid-phase Hugoniot data. X-ray-diffraction studies at ambient temperature[30,31,31a] showed that Na remains bcc up to at least 48 GPa,[31] which is the highest pressure reached so far in static compression experiments of Na.

The limited experimental information on the high-pressure polymorphism of Na contrasts with the variety of phase transitions known for the other alkali metals.[32] These metals also crystallize in the bcc structure at ordinary conditions. Phase transitions to fcc modifications have been observed for Li at 7.5 GPa,[33] K at 11.5 GPa,[34] Rb at 7 GPa,[35,36] and Cs at 2.3 GPa.[37] For the pretransition metals K, Rb, and Cs noncubic modifications were reported at higher pressures.[34,36,38–44]

Here we report results of a high-resolution monochromatic x-ray-diffraction study of Na under pressure at $T=298$ K. The primary motivations for this work were to explore the range of stability of the bcc phase and to take advantage of high-resolution synchrotron x-ray diffraction techniques to determine an accurate pressure-volume (PV) relation in the 100-GPa pressure range. For the pressures covered here, only one structural transition occurred, from bcc to fcc at 65(1) GPa. The fcc phase is found to be stable up to 103 GPa. At higher pressures we have observed phase transitions to several low-symmetry structures which will be discussed separately.[45] In the course of the experiments it was noted that Na may be a very good quasihydrostatic medium for diamond-anvil-cell (DAC) experiments at pressures up to at least 100 GPa. This aspect is possibly related to anomalies in the elastic (and mechanical) properties of bcc and fcc Na under pressure, as discussed in theoretical work.[11,46] The experimental data reported here are compared to results of total-energy calculations we performed with the full-potential linearized augmented-plane-wave (FLAPW) method and to other recent calculations of the equation of state and structural stability of Na.[11–13]

II. EXPERIMENTS

A. Experimental details

The x-ray-diffraction experiments were carried out at the undulator beamline ID9 of the European Synchrotron Radiation Facility using DAC's with the cell axis oriented along the x-ray beam. The diamond anvils had tips of 100- or 150-μm diameter and 9° bevels extending to diameters of 400–450 μm. The rhenium gaskets had initial hole diameters of 40 or 50 μm.

The Na samples were cut from a rod with a stated purity of 99.9%. Loading of samples into a DAC was performed under inert gas atmosphere. No pressure medium was used in order to avoid chemical reactions. A corrosive effect of Na on the diamond anvils, causing some difficulty in DAC experiments with Li,[5,9] was not noted. Data were collected in four runs, one to 86 GPa with a ruby chip as optical pressure sensor,[47] a second one to 69 GPa with ruby and Ta powder as pressure marker, and two runs to >100 GPa with a Ta

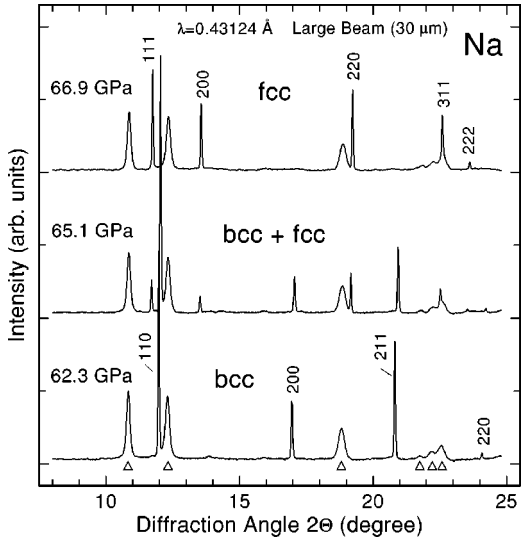

FIG. 1. Angle-dispersive synchrotron x-ray-diffraction diagrams of Na at pressures near 65 GPa ($\lambda = 0.43124$ Å). The sequence of diagrams is for the bcc phase (62.3 GPa), a mixed phase (65.1 GPa), and the fcc phase (66.9 GPa). These diagrams were measured with a relatively large beam diameter (30 μm), such that a large fraction of the sample contributes to the diffracted intensity. In this setting broad diffraction peaks from the rhenium gasket are seen also (marked by triangles). Note that the Bragg reflections of Na are much narrower than those of the strained gasket. In fact, the widths of Na diffraction lines were close to the instrumental resolution throughout the 100-GPa pressure range covered in the present experiments.

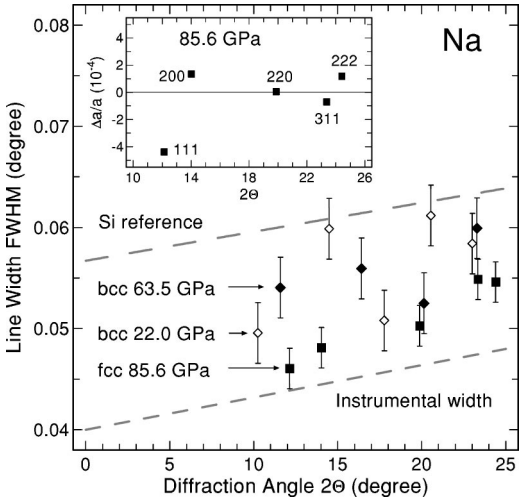

FIG. 2. Widths of Bragg reflections of Na at 22.0 GPa (bcc), 63.5 GPa (bcc), and 85.6 GPa (fcc), plotted as a function of diffraction angle ($\lambda = 0.43124$ Å). Error bars indicate the combined statistical errors and variations which depend on the choice of the peak profile function. The instrumental resolution limit is indicated as well as the typical dependence of the widths on 2Θ usually observed for a Si calibration sample at ambient pressure using the same experimental settings. The inset demonstrates the scatter of lattice constant values of fcc-Na at 85.6 GPa evaluated from individual reflections and normalized to the average lattice constant [$a = 3.5348(3)$ Å].

marker only. The ''ruby'' pressures are based on the 1986 scale.[48] The PV relation[49] used for Ta at 298 K was in part determined during the Na experiments, in part through independent measurements in a N_2 pressure medium. Details on the calibration of the Ta marker, which is based on the same ruby scale, are given elesewhere.[49]

X-ray-diffraction patterns were recorded on a flat image plate (MAR3450 system). Conventional diffraction diagrams were obtained by integration of the two–dimensional images using the FIT2D software.[50] Diffraction patterns of a Si reference sample were used in the calibration of the diffraction geometry. The x-ray wavelength varied between 0.41 and 0.45 Å in different runs. The sample to plate distance was ~ 360 mm. Two different beam diameters were used; with a small diameter of nominally ~ 10 μm it was possible to fully avoid the diffraction from the Re gasket, while for a beam diameter of 30 μm we obtained a better averaging over crystallite orientations.

B. Experimental results

Selected diffraction diagrams of Na measured at pressures between 62 and 67 GPa are shown in Fig. 1. A smooth background, arising mainly from the Compton scattering in diamond (see, e.g., Ref. 5), has been subtracted. The diagrams shown in Fig. 1 were measured with a large beam diameter of 30 μm, such that almost the entire sample contributes to the diffracted intensity. In this setting, broad reflections from the strained rhenium gasket are observed in addition to the very sharp reflections from the sample. At all pressures Na shows a strong tendency to recrystallize and it was not possible to obtain diffraction rings with homogeneous intensity distribution. After integration of the diffraction images the intensities approximately are as expected, but differences in relative reflection intensities of up to 50% occurred.

The structure of Na remains bcc up to 65 GPa. At this pressure diffraction peaks from a new phase appeared and at 66.9 GPa the bcc phase was not observed any more in the run shown in Fig. 1. The new phase of Na has a face-centered-cubic cell (see Bragg indices for the topmost pattern in Fig. 1). The bcc-fcc transition pressure (onset) is rather well defined; in different runs it occurred between 65 and 66 GPa. In one run a weak 110 reflection of the bcc phase was observed up to 70 GPa. The hysteresis in pressure of the transition was not explored for technical reasons (risk of breaking diamonds upon unloading).

It is important to note here that the Bragg reflections of Na showed no indication (within instrumental resolution) for deviatoric stresses. For both structures, bcc and fcc, the lattice constants from individual reflections differ by less than 0.02 % from the average value, with occasional observation of an outlier point (up to 0.05%, see, e.g., data for the fcc phase at 85.6 GPa shown in the inset of Fig. 2) probably due to the spotty nature of the diffraction patterns. Throughout the investigated pressure range, the widths of Na Bragg reflections stayed close to the instrumental resolution. This is illustrated in Fig. 2, which shows line width data for diffraction patterns taken at three different pressures. At all pressures the line widths of Na reflections do not exceed those of

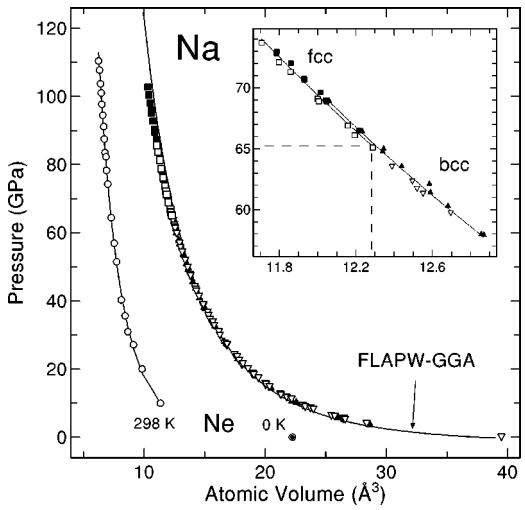

FIG. 3. Pressure-volume data for Na at $T=298$ K. Triangles are for the bcc phase and squares for the fcc phase. Open and closed triangles and squares are used for data based on pressure measurement by the ruby luminescence method and Ta marker, respectively. The solid line corresponds to a calculated PV relation for fcc-Na (see the text). The inset shows an expanded view covering the bcc-fcc phase-transition regime. Pressure-volume data of solid neon (Ref. 52), the neighboring closed-shell element of Na in the Periodic Table, are shown for comparison (closed and open circles).

the Si calibration sample at ambient pressure. For the Si sample the width is partly determined by the average particle size needed to obtain homogeneous intensity distributions on Debye-Scherrer rings. We note in Fig. 2 that the line widths for the fcc pattern taken at 85.6 GPa lie closest to the instrumental limit, which is largely determined by the resolution of the image plate. From the combined peak position and linewidth data we infer that macroscopic strain distributions and microstrains in the Na sample are below the detection limit of the present experiment. Taking into account the good instrumental resolution, one may infer that Na could be an excellent quasi-hydrostatic medium for x-ray diffraction studies.

The pressure vs atomic volume data of Na are shown in Fig. 3. The expanded view of the phase-transition regime in the inset to Fig. 3 demonstrates that the volume change at the bcc-fcc transition is extremely small. At the phase transition (for the 65.1-GPa diagram in Fig. 1) the lattice constants are 2.9073 Å ($V_{\rm atom}=12.2867$) and 3.6627 Å ($V_{\rm atom}=12.2841$) for the bcc and fcc phases, respectively. Several patterns showed bcc and fcc phases simultaneously. Taking the average of different observations, the relative volume difference $(V^{fcc}\text{-}V^{bcc})/V^{bcc}$ is only $-1(1)\times10^{-3}$, which is close to our resolution limit for the volume differences between two cubic phases. For comparison, at the bcc-fcc transition in Li near 7.5 GPa (298 K) the difference is also small: $-1.6(3)\times10^{-3}$.[5] At the phase transition the relative volume V/V_0 of Na is 0.31 and at the highest pressure (103 GPa) covered in this experiment it is 0.26. A discussion of microscopic bcc-fcc transformation mechanisms in Na is outside the scope of the present work. Regarding this aspect we just refer to recent theoretical treatments focusing on alkali metals.[21,51]

Neon is the closed-shell element next to Na in the Periodic Table. Experimental PV data for neon[52] are also shown in Fig. 3. At 100 GPa the atomic volume of Na is ~60% larger than that of Ne, and the nearest-neighbor Na-Na distance of 2.447 Å is slightly lower than the smallest distance within the stability range of the bcc phase (2.52 Å). The distances are significantly larger than twice the ionic radius of Na^+ (1.02 Å for a coordination number of 6). In a quite simplified picture it is the extra valence electron of Na which requires about 60% more volume compared to the neighboring closed shell system at the same pressure. The valence electrons of Na may play the role of a "lubricant," allowing for easy shear motion and possibly lower shear strength compared to Ne at the same pressure.

For fitting the PV data of Na, we use the $H02$ relation proposed by Holzapfel[53]

$$P=3B_0X^{-n}(1-X)\exp[(1.5B'-n+0.5)(1-X)],$$

with

$$X=(V/V_0)^{1/3} \quad \text{and} \quad n=5. \tag{1}$$

Here V_0, B_0, and B' are the volume, bulk modulus, and pressure derivative of the bulk modulus, respectively, at a reference pressure (usually ambient pressure). A choice $n=2$ in Eq. (1) would correspond to the relation of Vinet *et al.*[54] For the lattice constant of Na at ambient conditions we adopt the value $a_0=4.2908$ Å (Ref. 14) ($V_{\rm atom}=39.499$ Å^3). Since solid Na is highly compressible, differences in the a_0 values of the order 5×10^{-4} (Refs. 55 and 56) are not important for our data analysis. The results of a fit depend on the errors (weights) assigned to the individual data points. Except for systematic errors, there are mainly two sources of uncertainties: the pressure measurement and the lattice constant measurement. The latter can be mapped on the pressure axis. We use a global estimate where we assign an absolute error of 0.05 GPa and a relative error of 1.5% to each pressure value. In Table I we list the parameters B_0 and B' obtained by fitting Eq. (1) to the bcc and fcc phase data using the above error estimate.

Since the volume change at the bcc-fcc transition is extremely small, we have determined the parameters B_0 and B' for the combined bcc and fcc data. For this latter fit, in Fig. 4 we show the difference between data and fitted relation. There is hardly any indication of systematic trends in the differences. This means that Eq. (1) is fully adequate to describe the data within the full pressure range up to 100 GPa. It should be noted that our data for Na can be equally well described (in a least-squares sense) by a Birch (also termed third-order Birch-Murnaghan) equation[57] and the corresponding parameter values are similar to those obtained for Eq. (1). The only reason for not using the Birch relation would be that in some cases it is less well suited for extrapolations to small volumes.[58] Within the pressure range covered by the present measurements, however, Eq. (1) and the Birch relation are almost equivalent with respect to χ^2 minimization. For the Vinet relation [$n=2$ in Eq. (1)] the least-squares sum (χ^2) is about 50% larger and this is reflected in

TABLE I. Equation-of-state parameters for Na. The quantities V_0, B_0, and B' are the atomic volume, bulk modulus, and pressure derivative of the bulk modulus, all at ambient pressure unless noted otherwise. The experimental data are for room temperature, the parameters giving the best fit to our calculated pressure-volume relations for bcc- and fcc-Na (lower part of the table) are for the frozen-lattice limit. The parameters were obtained by fitting semi empirical PV relations to the data or calculated results. In the last column *H*02 refers to Eq. (1), ME to the Murnaghan equation, and BE to the Birch relation.

Source	Method	Phase	V_0 (Å^3)	B_0 (GPa)	B'	Relation
Ref. 29	Shock compr.	(liq)		6.15	3.74	*H*02
Ref. 24	Direct volume	bcc		6.131(5)	3.69(4)	ME
Ref. 25	Direct volume	bcc	39.426[a]	6.06(2)	4.125(40)	ME
Ref. 31	X-ray diffr.	bcc	39.43	6.06[b]	4.08(9)	*H*02
This work	X-ray diffr.	bcc	39.499[c]	6.310(80)	3.886(20)	*H*02
		fcc	39.499[c]	6.433(30)	3.83(8)	*H*02
		fcc	12.290(22)[d]	175.0(90)	2.20(60)	*H*02
		bcc+fcc	39.499[c]	6.368(60)	3.859(20)	*H*02
This work	FLAPW-GGA	bcc	37.7(2)	6.81(16)	3.93(1)	BE
	FLAPW-GGA	fcc	37.7(2)	6.85(18)	3.92(1)	BE
	FLAPW-LDA	fcc	33.42(3)	8.57(18)	3.95(1)	BE

[a]Volume V_0 at 294 K.
[b]Value adopted from Ref. 25.
[c]Volume V_0 at 298 K from Ref. 14.
[d]Volume V_0 at 65.1 GPa.

the corresponding difference plot in Fig. 4. The Murnaghan relation[59] is not suitable to fit our data.

The dependence of the bulk modulus of bcc and fcc Na on volume is shown in Fig. 5. At 100 GPa the bulk modulus (250 GPa) has increased by a factor of about 40 compared to ambient, and is more than half of that of diamond at ambient. The slope $\beta(V) = -d \ln B/d \ln V$ clearly decreases with decreasing volume. The assumption of a volume-independent parameter β is not valid for highly compressed Na.

C. Comparison with other *PV* data for Na

In Fig. 6 we compare our B_0 and B' values with results derived from volumetric methods[22–25] and ultrasonic experiments.[26,27] The two solid lines indicate the correlation of our parameter values for the bcc phase [Eq. (1) and the Birch relation]. Our fitted B_0 and B' values fall into the parameter field spanned by the various experimental results; the closest match is with the ultrasonic data of Martinson *et al.*[27] This overall consistency is somewhat fortuitous, be-

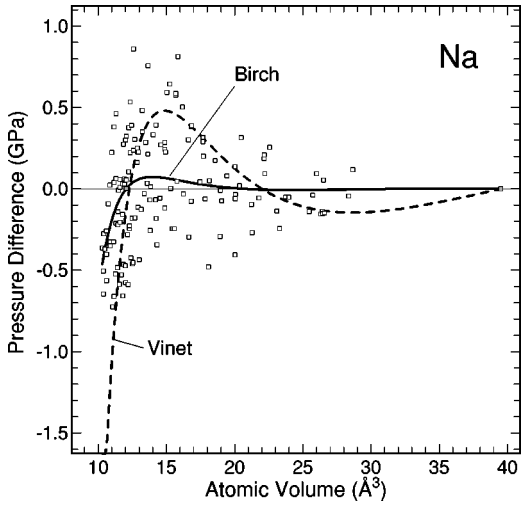

FIG. 4. Difference between measured pressures and pressures calculated from the fitted PV relation [Eq. (1)] (represented by open squares). Also shown are the corresponding differences for fitted Birch and Vinet relations relative to the fit using Eq. (1).

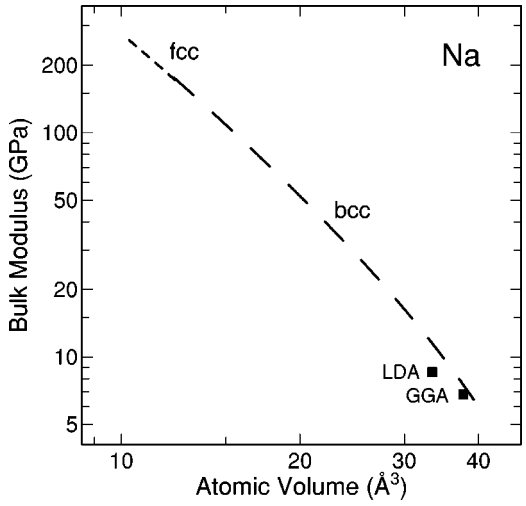

FIG. 5. Bulk modulus of Na as a function of atomic volume derived from the fitted PV relations [Eq. (1)] for the bcc and fcc phases. Symbols represent calculated bulk modulus values at ambient pressure obtained from total energy calculations using the LDA and GGA approximations (see the text).

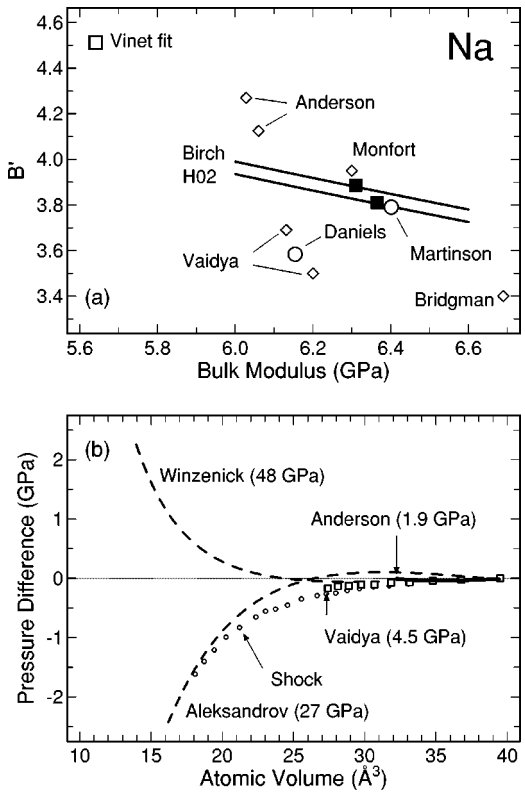

FIG. 6. (a) Pairs of B_0 (bulk modulus at ambient) and B' (pressure derivative of the bulk modulus) values for bcc Na from different experiments represented in a two-dimensional plot. Filled squares: present parameter values from *H*02 and Birch fits; solid lines: correlation between B_0 and B' for these fits; open square: from the Vinet fit of the present data; open diamonds: volumetric data (Refs. 22–25); open circles: from ultrasonic data (Refs. 26 and 27). (b) Difference plot for volumetric (Refs. 24 and 25), x-ray diffraction (Refs. 30 and 31), and reduced shock data (Ref. 29) of Na relative to the present PV relation.

cause we would not expect that a two-parameter PV relation giving the best *average* description over a very large pressure (volume) range also closely matches the low-pressure results. The consistency simply means that the *H*02 and Birch relations are well suited to describe the compression behavior of Na over a wide range of pressure and density.

The differences between previous static and reduced shock compression data of Na and our fitted PV relation are also indicated in Fig. 6. For the volumetric data,[24,25] the maximum difference in pressure is 0.15 GPa. The two previous x-ray-diffraction studies[30,31] showed deviations in opposite directions, up to ± 2.5 GPa. If the pressure values of Aleksandrov *et al.*[30] are updated to the 1986 ruby scale, the deviation would become smaller. The pressure difference to reduced ($T=298$ K) shock data[29] does not exceed 2 GPa. As already mentioned, the shock data are mostly for the liquid phase.

The ambient-pressure bulk modulus and its pressure derivative enter into the macroscopic description of low-pressure thermal properties. Since the values of B_0 and B' obtained here are basically consistent with earlier results, there is no need to repeat the standard treatment of anharmonic effects, usually discussed within the quasi-harmonic Mie-Grüneisen approximation.[25,52] The thermodynamic properties of highly compressed Na appear to be an interesting subject for further investigations.

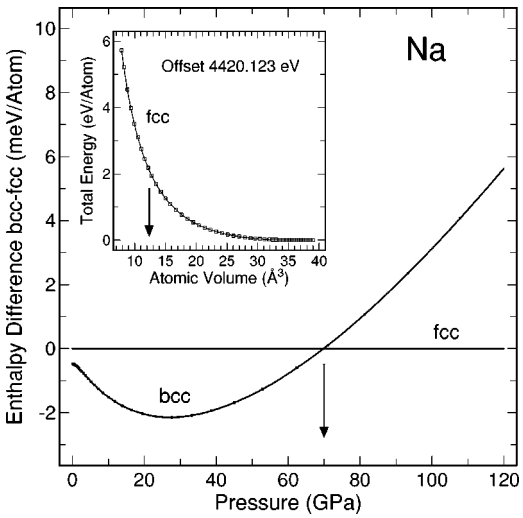

FIG. 7. Calculated enthalpy difference for bcc and fcc phases of Na as a function of calculated pressure (FLAPW-GGA calculations). The inset shows the calculated total energy as a function of atomic volume (covering the pressure range up to ~200 GPa). Arrows mark the pressure and volume of the bcc-fcc transition.

III. CALCULATIONS

A. Theoretical Method

We have performed total energy calculations for Na using the FLAPW method as implemented in the WIEN97 code.[60] The method is based on *first-principles* density-functional theory. In the case of alkali metals the generalized gradient approximation (GGA) for the exchange-correlation energy was shown to be superior to the local-density approximation (LDA), if judged, for instance, by the agreement with ambient pressure lattice constants.[61,62] We have performed calculations using mainly the GGA.[63] Scalar relativistic corrections were included. The convergence of the calculated results was checked with respect to the plane-wave basis set and the *k*-point sampling within the irreducible part of the Brillouin zone (BZ). The plane-wave cutoff K_{max} was determined by $R_{MT} \cdot K_{max} = 9.0$ (R_{MT} is the muffin-tin radius) and 165 points were used for the *k*-point sampling in the irreducible wedge of the Brillouin zone. The Na 2*s* and 2*p* states were treated as valence states using the local orbital extension of the FLAPW method.[60]

B. Calculated structural stability

Total energies of the bcc and fcc phases were calculated for about 30 volumes from 40 Å^3/atom down to 8 Å^3/atom. The inset to Fig. 7 shows the volume dependence of $E_{\rm tot}$ for the fcc phase. On the scale used in the figure, the results for the bcc phase are indistinguishable from those for the fcc phase. The equilibrium atomic volumes corresponding to the minima in total energies $E_{\rm tot}$ are

37.7(2) Å^3 for the bcc and fcc structures. From the extrapolation of temperature-dependent lattice constant data at ambient pressure,[56] the atomic volume at $T=0$ K is 37.74 Å^3. The effect of zero-point motion on the equilibrium volume of Na can be estimated within the quasiharmonic approximation.[25,64] The isochoric zero-point lattice dynamical contribution to the pressure is ~ 0.08 GPa.[25] The corresponding volume difference between $T=0$ K and static-lattice volume is -0.38 Å^3. Thus the calculated equilibrium volume differs by only $+1\%$ from the ''experimental'' static-lattice volume of 37.36 Å^3.

The difference in total energy for the bcc and fcc structures was calculated to be only 0.3 meV per atom at equilibrium, favoring the bcc structure. This small energy difference lies within the uncertainty of the calculation which is estimated to be of the order of 1 meV/atom.

The pressure-volume relation for the static lattice case is obtained according to $P(V)=-dE_{tot}(V)/dV$. Instead of applying a numerical differentiation, we have fitted the calculated $E_{\rm tot}(V)$ data by the $E(V)$ expression corresponding to the Birch relation (solid line in the inset of Fig. 7). In this way we obtain the calculated values of B_0 and B' listed in Table I.

The $E_{\rm tot}(V)$ and $P(V)$ relations enter into the calculation of the enthalpy $H=E_{\rm tot}+PV$. According to the calculated enthalpy differences (Fig. 7) increasing pressure first stabilizes bcc, but then, near 70 GPa, the bcc structure becomes unstable relative to the fcc structure. The calculated transition pressure of 70 GPa for the static-lattice case (having an estimated uncertainty of ± 10 GPa) agrees well with the experimental results at 298 K. The bcc-fcc phase-transition pressure may have a rather weak temperature dependence, similar to the results for potassium.[11]

Structural phase transitions in Na, considering the common close-packed structures bcc, fcc, and hcp, have been studied in several total energy calculations using a variety of theoretical methods; see, e.g., Refs. 11–13 and 64–67. At ambient pressure, different results are reported for the relative ordering of phases, but the total-energy differences are extremely small, close to the estimated uncertainties of the calculations. Calculations in which the effect of pressure on the relative stability of bcc and fcc structures was considered indicate a behavior which is qualitatively similar to that shown in Fig. 7. In recent reports[11–13] the calculated bcc-fcc transition pressure ranges from 70 to 95 GPa, depending on the calculational method and the approximations for the exchange-correlation potential and energy. In view of the small energy differences involved it is probably fair to say that, in general, most of the *first-principles* calculations for Na place the pressure-induced bcc-fcc transition at approximately the correct volume and differences in calculated transition pressures should not be overemphasized.

C. Calculated pressure-volume relations

The calculated pressure-volume relation for the fcc phase of Na is compared in Fig. 3 to the experimental data. At 100 GPa (experimental volume 10.4 Å^3) the calculated volume is larger by $\sim 3\%$. This could be considered as an excellent agreement which looks even better when given as a 1% difference in lattice parameter. This also applies to the full potential linear-muffin-tin-orbital calculations for Na by Christensen and Novikov,[13] who obtained very similar PV curves.

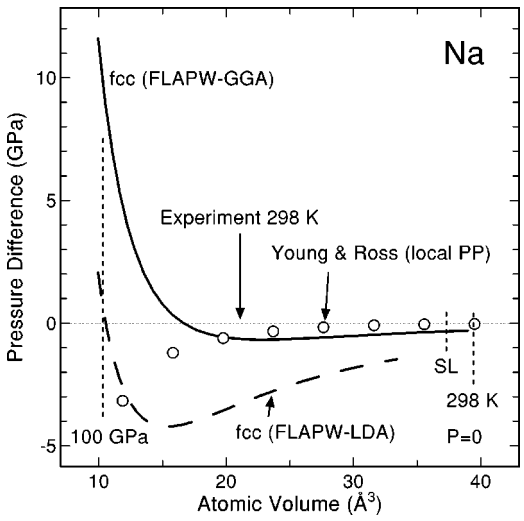

FIG. 8. Plotted as a function of the atomic volume of Na are the difference between calculated pressures and ''experimental'' pressures (i.e., the pressures given by the PV relation fitted to the present experimental data). The solid and dashed lines represent results of FLAPW calculations for the fcc phase using different approximations (GGA and LDA) for the exchange-correlation potential and energy (see the text). The results for the bcc phase (not shown) hardly differ from those for the fcc phase. The results of a local-pseudopotential calculation (Refs. 69) are shown for comparison.

Figure 8 shows the pressure difference between calculated and experimental pressures for the fcc structure (again the bcc structure is hardly different from the fcc structures). At ambient density the difference for the GGA results is negative because the calculations are for the static lattice case. The GGA difference first is nearly constant with increasing compression (it should decrease slightly because of decreasing zero-point and thermal pressure) and then near $V_{\rm atom}$ ~ 16 Å^3 (30 GPa) the calculated PV curve crosses through the experimental data measured at 298 K. At the volume corresponding to an experimental pressure of 100 GPa the calculated pressure (GGA) is larger by ~ 10 GPa (thermal pressure contributions are negligible on this scale). Thus it is in terms of pressure at a given volume, that the agreement between FLAPW-GGA calculations and experiment may be viewed as unsatisfactory. This is not restricted to highly compressible Na. For instance, Ta appears to be another example of an elemental metal where results of GGA calculations[68] agree well with ambient pressure bulk properties but yield pressures slightly too high at around 100 GPa when compared to *static* experimental data.

For comparison, in Fig. 8 we also show the result of a FLAPW calculation performed with the LDA (see the corresponding parameters given in Table I). At ambient pressure the LDA volume is 11% smaller compared to the GGA volume, but this difference decreases to 3% at 100 GPa. In other words, at 100 GPa the LDA calculation matches almost ex-

actly the experimental volume (and pressure). The result of a local pseudopotential calculation[69] is also shown in Fig. 8.

The volume/pressure difference between GGA results and the experimental data near 100 GPa may indicate that binding is underestimated (repulsion overestimated) in the GGA calculation for Na at high densities. However, we also have to ask whether this difference may in part be due to systematic errors in the ruby pressure scale.[48] This scale has undergone several tests (see, e.g., Refs. 52 and 70), and is considered to be quite robust. About a 10% difference in pressure would be difficult to reconcile with the stated uncertainty (5%) of shock wave data, on which the ruby scale is based, unless there are systematic errors in the experimental procedures used for the ruby calibration, possibly arising from non hydrostatic stresses.

It has been suggested that *first-principles* calculations of the PV relation of Na could provide a pressure standard,[11,30] replacing shock wave data of other metals in the calibration of pressure sensors like ruby. This would be a very attractive route, because Na offers a combination of high compressibility (at least for low and intermediate pressures) and good quasi-hydrostatic properties up to at least 100 GPa. Microscopic (*first-principles*) theory was shown to reproduce well the high-pressure isotherms of several metals, usually derived from a combination of experimental Hugoniot data and thermodynamic relations. If this is also valid for the FLAPW-GGA calculations of Na, the present experimental and calculated results would demonstrate the need for a correction of the ruby scale in a manner similar to what has been proposed earlier[71] based on the pressure dependence of the first-order Raman mode of diamond.

IV. CONCLUSIONS

The conclusions from the present work are as follows.

(1) We observed a bcc-to-fcc structural transition in Na at 65 GPa. The pressure-induced bcc-fcc transition is therefore common to all alkali metals at room temperature. What is special about Na is that a rather high compression is required ($V/V_0 = 0.31$) compared to Li and the heavy (pretransition) alkali metals K, Rb, and Cs. The bcc-fcc transition pressure for Na calculated within the FLAPW-GGA scheme is close to the experimental value. This also applies to several other *first-principles* calculations reported in the literature.

(2) The pressure-volume relation of Na has been determined up to 103 GPa, the upper stability limit of the fcc phase. The pressures were determined directly by the ruby luminescence method or from the lattice constant of a Ta marker. The PV relation of Ta used here[49] is based on the same ruby scale. Near 100 GPa we find a difference of +10% in pressure between the PV relation calculated within the FLAPW-GGA scheme and experimental data. The theoretical method employed here gives almost the correct volume at ambient but appears to underestimate binding (or overestimate repulsion) at high density.

(3) The difference between calculated PV relation and experiment also brings up a question about possible systematic errors in ruby-based pressure measurements in the 100-GPa range. The true pressures may be higher than obtained by the ruby method. This is not very relevant at moderate pressures of, say, 20–30 GPa, but would not be negligible at 100 GPa and above.

(4) The observations made in this study indicate that Na would be an excellent quasi-hydrostatic pressure medium for DAC x-ray-diffraction studies at pressures beyond 50 GPa. Of course, it can be considered only if its chemical reactivity does not cause any problems. Exploring in more detail the elastic and mechanical properties of Na under pressure would be a worthwhile project. This would involve diffraction experiments in a different geometry[72,73] than used in this work.

(5) A revised (improved) ruby pressure scale could possibly be established, based on DAC x-ray-diffraction experiments of a suitable metal placed in a Na medium and loaded together with ruby, combined with simultaneous Raman measurements of diamond grains. Theory would have to come up with identifying the ''best'' PV relations for the two metals and the ''best'' phonon frequency calculations for diamond. Consistency with reduced shock data (or vice versa) would be a boundary condition.

ACKNOWLEDGMENTS

The authors thank M. Amboage for help in the initial stage of the experiments. Useful discussions with N. E. Christensen, N. W. Ashcroft, and J. B. Neaton are acknowledged.

*Corresponding author. Email address: k@syassen.de

[1] J.B. Neaton and N.W. Ashcroft, Nature (London) **400**, 141 (1999).
[2] J.C. Boettger and S.B. Trickey, Phys. Rev. B **32**, 3391 (1985).
[3] W.G. Zittel, J. Meyer-ter-Vehn, J.C. Boettger, and S.B. Trickey, J. Phys. F: Met. Phys. **15**, L247 (1985).
[4] F. Siringo, R. Pucci, and G.G.N. Angilella, High Press. Res. **15**, 255 (1997).
[5] M. Hanfland, I. Loa, K. Syassen, U. Schwarz, and K. Takemura, Solid State Commun. **112**, 123 (1999).
[6] V.V. Struzhkin, R.J. Hemley, and H.K. Mao, Bull. Am. Phys. Soc. **44**, 1489 (1999).
[7] Y. Mori and A. Ruoff, Bull. Am. Phys. Soc. **44**, 1489 (1999).
[8] V.E. Fortov, V.V. Yakushev, K.L. Kagan, I.V. Lomonosov, V.I. Postov, and T.I. Yakusheva, Pis'ma Zh. Éksp. Teor. Fiz. **70**, 620 (1999) [JETP Lett. **70**, 628 (1999)]; V.E. Fortov, V.V. Yakushev, K.L. Kagan, I.V. Lomnosov, V.I. Postov, T.I. Yakusheva, and A.N. Kuryanchik, *ibid.* **74**, 458 (2001) [*ibid.* **74**, 418 (2001)].
[9] M. Hanfland, K. Syassen, N.E. Christensen, and D.L. Novikov, Nature (London) **408**, 174 (2000).
[10] E. Wigner and F. Seitz, Phys. Rev. **43**, 804 (1933); **46**, 509 (1934)
[11] M.I. Katsnelson, G.V. Sinko, N.A. Smirnov, A.V. Trefilov, and K.Yu. Khromov, Phys. Rev. B **61**, 14420 (2000).
[12] J.B. Neaton and N.W. Ashcroft, Phys. Rev. Lett. **86**, 2830 (2001).
[13] N.E. Christensen and D.L. Novikov, Solid State Commun. **119**, 477 (2001).

[14] C.S. Barrett, Acta Crystallogr. **9**, 671 (1956).
[15] V.G. Vaks, J. Phys.: Condens. Matter **1**, 5319 (1989).
[16] R. Berliner, O. Fajen, H.G. Smith, and R.L. Hittermann, Phys. Rev. B **40**, 12086 (1989).
[17] H.G. Smith, R. Berliner, J.D. Jorgensen, and J. Trivisonno, Phys. Rev. B **43**, 4524 (1991).
[18] R. Berliner, H.G. Smith, J.R.D. Copley, and J. Trivisonno, Phys. Rev. B **46**, 14436 (1992).
[19] W. Schwarz, O. Blaschko, and I. Gorgas, Phys. Rev. B **46**, 14448 (1992).
[20] H. Abe, K. Ohshima, T. Suzuki, S. Hoshino, and K. Kakurai, Phys. Rev. B **49**, 3739 (1994).
[21] O. Blaschko, V. Dmitriev, G. Krexner and P. Tolédano, Phys. Rev. B **59**, 9095 (1999).
[22] P.W. Bridgman, Phys. Rev. **60**, 351 (1941); P.W. Bridgman, Proc. Natl. Acad. Sci. U.S.A. **76**, 55 (1948).
[23] C.E. Monfort and C.A. Swenson, J. Phys. Chem. B **26**, 623 (1965).
[24] S.N. Vaidya, I.C. Getting, and G.C. Kennedy, J. Phys. Chem. Solids **32**, 2545 (1971).
[25] M.S. Anderson and C.A. Swenson, Phys. Rev. B **28**, 5395 (1983).
[26] W.B. Daniels, Phys. Rev. **119**, 1246 (1960).
[27] R.H. Martinson, Phys. Rev. **178**, 802 (1969).
[28] C.S. Zha and R. Boehler, Phys. Rev. B **31**, 3199 (1985).
[29] G.C. Kennedy and R.N. Keeler, in *AIP Handbook*, edited by D. E. Gray (McGraw-Hill, New York 1972), p. 4–99.
[30] I.V. Aleksandrov, V.N. Kachinskii, I.N. Makarenko, and S.M. Stishov, Pis'ma Zh. Éksp. Toer. Fiz. **36**, 336 1982 [JETP Lett. **36**, 411 (1982)].
[31] M. Winzenick, PhD thesis, Universität Paderborn, 1996.
[31a] J.N. Fritz and B. Olinger, J. Chem. Phys. **80**, 2864 (1984).
[32] D.A. Young, *Phase Diagrams of the Elements* (University of California Press, Berkeley, 1991).
[33] B. Olinger and W. Shaner, Science **219**, 1071 (1983).
[34] K. Takemura and K. Syassen, Phys. Rev. B **28**, 1193 (1983).
[35] K. Takemura and K. Syassen, Solid State Commun. **44**, 1161 (1982).
[36] H. Olijnyk and W.B. Holzapfel, Phys. Lett. **99A**, 381 (1983).
[37] H.T. Hall, L. Merrill, and J.D. Barnett, Science **146**, 1297 (1964).
[38] K. Takemura, S. Minomura, and O. Shimomura, Phys. Rev. Lett. **49**, 1772 (1982).
[39] H. Tups, K. Takemura, and K. Syassen, Phys. Rev. Lett. **49**, 1776 (1982).
[40] M. Winzenick, V. Vijayakumar, and W.B. Holzapfel, Phys. Rev. B **50**, 12381 (1994).
[41] U. Schwarz, K. Takemura, M. Hanfland, and K. Syassen, Phys. Rev. Lett. **81**, 2711 (1998).
[42] U. Schwarz, K. Syassen, A. Grzechnik, and M. Hanfland, Solid State Commun. **112**, 319 (1999).
[43] U. Schwarz, A. Grzechnik, K. Syassen, I. Loa, and M. Hanfland, Phys. Rev. Lett. **83**, 4085 (1999).
[44] K. Takemura, N.E. Christensen, D.L. Novikov, K. Syassen, U. Schwarz, and M. Hanfland, Phys. Rev. B **61**, 14399 (2000).
[45] M. Hanfland, K. Syassen, N. E. Christensen, and D. L. Novikov, (unpublished).
[46] V.G. Vaks, J. Phys.: Condens. Matter **3**, 1409 (1991).
[47] G.J. Piermarini, S. Block, J.D. Barnett, and R.A. Forman, J. Appl. Phys. **46**, 2774 (1975).
[48] H.K. Mao, J. Xu, and P.M. Bell, J. Geophys. Res. **91**, 4673 (1986).
[49] M. Hanfland, K. Syassen, and J. Köhler, J. Appl. Phys. **91**, 4143 (2002).
[50] A.P. Hammersley, S.O. Svensson, M. Hanfland, A.N. Fitch, and D. Häussermann, High Press. Res. **14**, 235 (1996).
[51] V.L. Sliwko, P. Mohn, K. Schwarz, and P. Blaha, J. Phys.: Condens. Matter **8**, 799 (1996).
[52] R.J. Hemley, C.S. Zha, A.P. Jephcoat, H.K. Mao, and L.W. Finger, Phys. Rev. B **39**, 11820 (1989).
[53] W.B. Holzapfel, Europhys. Lett. **16**, 67 (1991).
[54] P. Vinet, J. Ferrante, J.R. Smith, and J.H. Rose, J. Phys. C **19**, L467 (1986).
[55] W. Adlhart, G. Fritsch, A. Heidemann, and E. Lüscher, Phys. Lett. **47A**, 91 (1974).
[56] H. Abe, K. Ohshima, T. Suzuki, and Y. Watanabe, J. Appl. Crystallogr. **27**, 1040 (1994).
[57] F. Birch, J. Geophys. Res. **83**, 1257 (1978), and references therein.
[58] W.B. Holzapfel, Rep. Prog. Phys. **59**, 29 (1996).
[59] F.D. Murnaghan, Proc. Natl. Acad. Sci. U.S.A. **50**, 244 (1944).
[60] P. Blaha, K. Schwarz, and J. Luitz, WIEN97, A Full Potential Linearized Augmented Plane Wave Package for Calculating Crystal Properties (Karlheinz Schwarz, Techn. Universität Wien, Austria 1999), ISBN 3-9501031-0-4. [Improved and updated Unix version of the original copyrighted code WIEN, which was published by P. Blaha, K. Schwarz, P. Sorantin, and S. B. Trickey, Comput. Phys. Commun. **59**, 339 (1990).]
[61] J.P. Perdew, J.A. Chevary, S.H. Vosko, K.A. Jackson, M.R. Perderson, D.J. Singh, and C. Fiolhais, Phys. Rev. B **46**, 6671 (1992).
[62] J.E. Jaffe, Z. Lin, and A.C. Hess, Phys. Rev. B **57**, 11834 (1998).
[63] J.P. Perdew, S. Burke, and M. Ernzerhof, Phys. Rev. Lett. **77**, 3865 (1996).
[64] M.M. Dacorogna and M.L. Cohen, Phys. Rev. B **34**, 4996 (1986).
[65] J.A. Moriarty and A.K. McMahan, Phys. Rev. Lett. **48**, 809 (1982).
[66] A.K. McMahan and J.A. Moriarty, Phys. Rev. B **27**, 3235 (1983).
[67] H.L. Skriver, Phys. Rev. B **31**, 1909 (1985).
[68] P. Söderlind and J.A. Moriarty, Phys. Rev. B **57**, 10340 (1998).
[69] D.A. Young and M. Ross, Phys. Rev. B **29**, 682 (1984).
[70] C.S. Zha, H.K. Mao, and R.J. Hemley, Proc. Natl. Acad. Sci. U.S.A. **97**, 13494 (2000).
[71] I.V. Aleksandrov, A.F. Goncharov, A.N. Zisman, and S.M. Stishov, Zh. Éksp. Teor. Fiz. **93**, 680 1987 [Sov. Phys. JETP **66**, 384 (1987)].
[72] A.K. Singh, H.-K. Mao, J. Shu, and R.J. Hemley, Phys. Rev. Lett. **80**, 2157 (1998), and references therein.
[73] T.S. Duffy, G. Shen, D.L. Heinz, J. Shu, Y. Ma, H.K. Mao, R.J. Hemley, and A.K. Singh, Phys. Rev. B **60**, 15063 (2000).